Salazar, P., Kummerow, J., Wigger, P., Shapiro, S., Asch, G. (2016): State of stress and crustal fluid migration related to west-dipping structures in the slab-forearc system in the northern Chilean subduction zone. - *Geophysical Journal International*, *208*, 3, pp. 1403—1413.

DOI: http://doi.org/10.1093/gji/ggw463

Geophysical Journal International

Geophys. J. Int. (2017) **208,** 1403–1413
Advance Access publication 2016 December 9
GJI Seismology

doi: 10.1093/gji/ggw463

State of stress and crustal fluid migration related to west-dipping structures in the slab-forearc system in the northern Chilean subduction zone

P. Salazar,[1,2,*] J. Kummerow,[3] P. Wigger,[3] S. Shapiro[3] and G. Asch[4]

[1]*Departamento de Ciencias Geológicas, Universidad Católica del Norte, Antofagasta, Chile. E-mail: pasalaz@ucn.cl*
[2]*National Research Center for Integrated Natural Disasters Management (CIGIDEN), Chile*
[3]*Freie Universität Berlin, Fachrichtung Geophysik, Berlin, Germany*
[4]*Helmholtz-Zentrum Potsdam, Deutsches GeoForschungsZentrum GFZ, Potsdam, Germany*

Accepted 2016 December 6. Received 2016 December 2; in original form 2016 May 27

SUMMARY

Previous studies in the forearc of the northern Chilean subduction zone have identified important tectonic features in the upper crust. As a result of these works, the West Fissure Fault System (WFFS) has recently been imaged using microseismic events. The WFFS is the westward-dipping, sharp lower boundary of the northern Chilean forearc and is geometrically opposed to subduction of the Nazca plate. The present article builds on this previous work and is novel in that it characterizes this structure's stress distribution using focal mechanisms and stress tensor analysis. The results of the stress tensor analysis show that the state of stress in the WFFS is related to its strike-slip tectonic context and likely represents a manifestation of local forces associated with the highest areas in the Andes. Two seismic clusters have also been identified; these clusters may be associated with a blind branch of the WFFS. We studied these clusters in order to determine their sources and possible connection with fluid migration across the upper plate. We observed that the two clusters differ from one another in some regards. The central cluster has characteristics consistent with an earthquake swarm with two clearly identifiable phases. Conversely, the SW cluster has a clear main shock associated with it, and it can be separated into two subclusters (A and A′). In contrast, similarities among the two clusters suggest that the clusters may have a common origin. The *b*-values for both clusters are characteristic of tectonic plate boundaries. The spatial spreading, which is approximately confined to one plane, reflects progressive growth of the main fracture underlying the swarm and subcluster A. We also find that earthquakes themselves trigger aftershocks near the borders of their rupture areas. In addition, the spatio-temporal migration of hypocentres, as well as their spatial correlation with areas that are interpreted to be fluid migration zones, suggest that there is a close relationship between fluid movement and the earthquake sources associated with the swarm and subcluster A. These observations point to stick-slip behaviour of the rupture propagation, which can be explained by earthquake-induced stress transfer and fluid flow in a fluid-permeated, critically loaded fault zone.

Key words: Seismicity and tectonics; Subduction zone processes; Crustal structure; South America.

1 INTRODUCTION

The convergence between the Nazca and South American plates is a subduction zone with relative plate motion oblique to the trench. This convergence is responsible for the Earth's longest and highest active mountain chain formed at an ocean-continent subduction margin, the Andes. The elevation and crustal thickness of this mountain range have mainly been produced by crustal shortening caused by the interaction between these plates. These characteristics cause the development of strike-slip fault systems in the overriding plate as a consequence of strain partitioning (Jarrard 1986a,b), and these fault systems are classified as 'trench-linked strike-slip faults' (Woodcock 1986). Two large-scale, margin-parallel shear zones have formed during convergence of the Nazca and South American tectonic plates in the northern Chilean Andean orogen: the Atacama Fault System (AFS) and the Precordillera Fault System (PFS). These huge structures are likely the surface manifestations

* Former Ph.D. student Freie Universität Berlin.

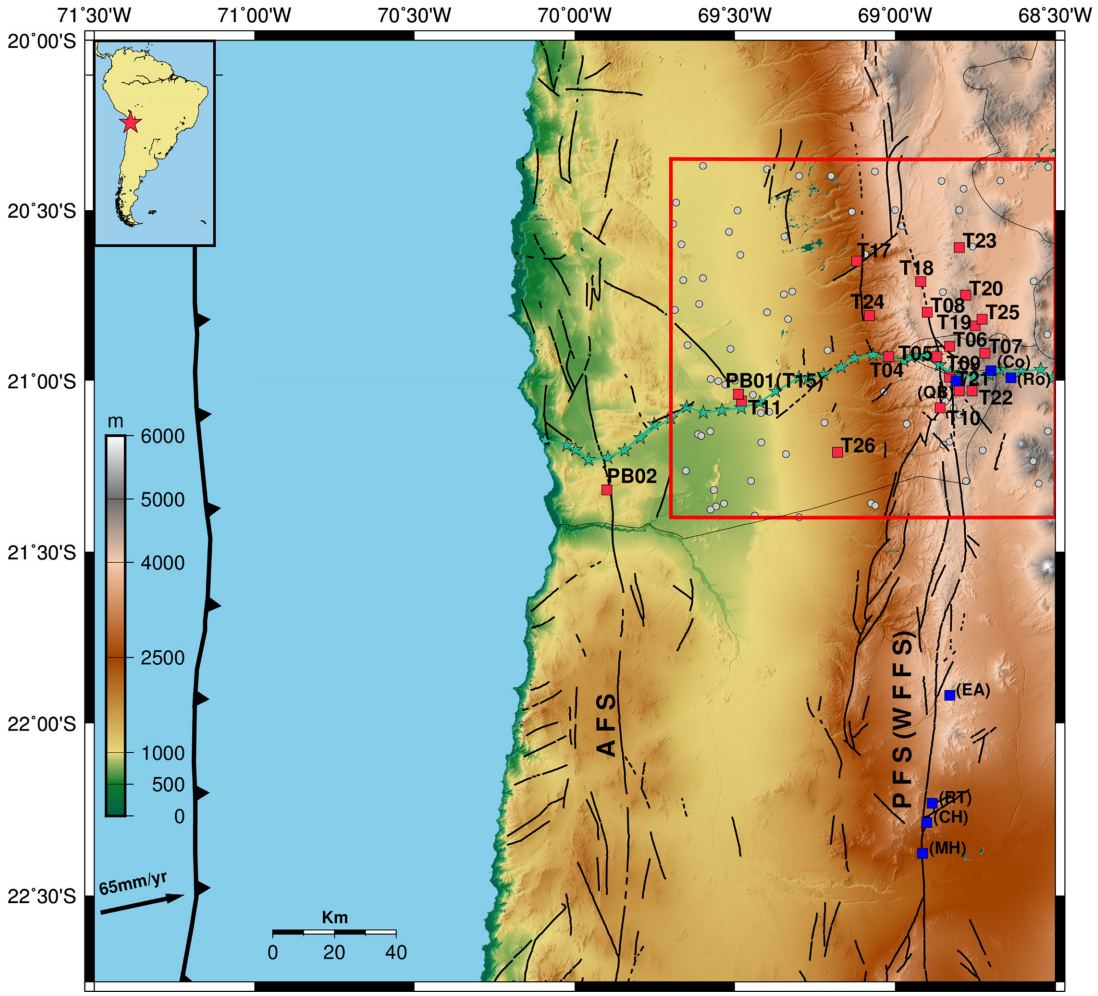

Figure 1. Local short-period network around the West Fissure Fault System (WFFS). On the map the station locations are shown as red squares. PB01 and PB02 are broad-band stations from the IPOC network; PB01 is in the same place as T15. The W–E crooked green line indicates the ANCORP profile with shot points (green stars). The blue squares indicate porphyry-copper deposits (MH: Ministro Hales, CH: Chuquicamata, RT: Radomiro Tomic, EA: El Abra, QB: Quebrada Blanca, Co: Collaguasi, Ro: Rosario). The black lines indicate the Atacama Fault System (AFS), the Precordillera Fault System (PFS) and the West Fissure Fault System (WFFS). Grey circles show the background seismicity between 1964/02 and 2009/11, as obtained from the IRIS catalogue (http://service.iris.edu/fdsnws/event/1/). The boundaries of the study area are indicated by red lines.

of complete partitioning of the strain, in which the plate interface accommodates pure thrust faulting and all of the trench-parallel component of the plate convergence is taken up within the upper plate and focused as shear stress within these strike-slip fault systems (Hoffmann-Rothe *et al.* 2006).

One of the more important features of the northern part of Chile is the Andean Precordillera. This region represents a morphostructural block that constitutes the western limit of the Altiplano. The uplift of this block was accomplished by fault motion along the PFS, which is traceable for more than 1000 km parallel to the N–S trending continental plate margin or subduction trench (Lindsay *et al.* 1995). The PFS not only played an important role in construction of the Altiplano but also influenced the emplacement and mineralization of some of the largest porphyry copper-related intrusions, which are called 'world-class deposits' by the economic geology community. The PFS is composed of various regional segments, each of which has undergone a distinct series of deformation events (Lindsay *et al.* 1995). In the northern part of Chile, the regional branch of the PFS is known as the West Fissure Fault System (WFFS), which is continuously exposed along a 170-km-long zone extending from Chuquicamata northward to Quebrada Blanca (both of which are world-class porphyry copper deposits; see Fig. 1).

The WFFS is a very dynamic regional fault zone. Geological evidence shows that focused hydrothermal activity has occurred there, at least intermittently, over millions of years. This hydrothermal activity is likely the primary reason why Chuquicamata and other porphyry copper deposits accumulated as much metal and sulphur as they did (Ossandón *et al.* 2001). The WFFS has been active since the Late Eocene/Early Oligocene (Reutter *et al.* 1996). Most authors assume that an older dextral strike-slip motion caused by subduction-related magmatic arc tectonics of the Incaic tectonic phase was followed by sinistral shear corresponding to a time of reduced convergence rate (Reutter *et al.* 1996). The youngest event is the reactivation of dextral slip under the same kinematic conditions as applied during the older phase. Tectonic inversion of the fault system is also reflected by varying amounts of displacement (dextral displacement: 0.5–2 km, sinistral displacement: 35–37 km; Reutter *et al.* 1991; Tomlinson & Blanco 1997a,b).

Because both the AFS and PFS can generally be traced for several hundred or even thousands of kilometres, it is believed that

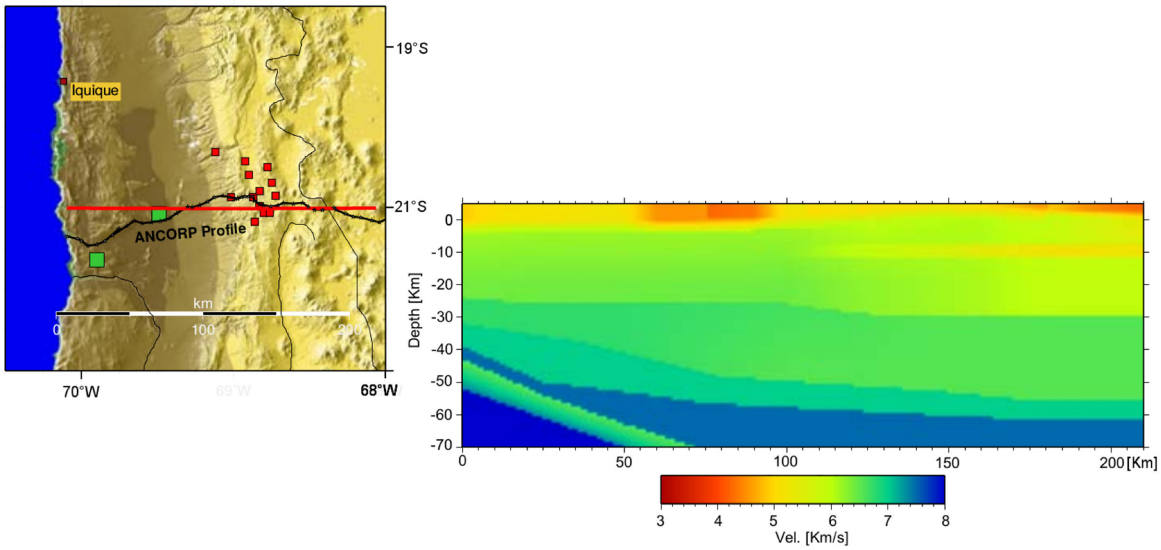

Figure 2. The 2-D *P*-velocity model by Lüth (2000). In the left panel, the straight red line indicates the position of the velocity model, the black line and crosses indicate the ANCORP profile, the red squares indicate short-period stations from the WFFS network, and the green squares indicate broad-band stations from the IPOC network. The right panel shows the cross-section view of the 2-D *P*-velocity model. Colours indicate different velocities (see the colour bar).

they may extend through the entire thickness of the lithosphere (Sylvester 1988). Previous studies of these zones have focused on intermediate-depth seismicity associated with subduction of the Nazca Plate beneath the South American Plate (e.g. Haberland & Rietbrock 2001; Heit 2005), the Tarapacá earthquake on 2005 June 13 (Peyrat *et al.* 2006; Delouis & Legrand 2007), the Aroma earthquake on 2001 July 24 (Legrand *et al.* 2007), intracontinental seismicity associated with the Central Andes Orocline (David 2007) and tectonic evidence of the western Altiplano plateau (e.g. Janssen *et al.* 2002; Victor *et al.* 2004; Farías *et al.* 2005).

Despite the geological, tectonic and economic importance of these fault zones, deep understanding of the seismic activity associated with these large tectonic structures, and the depth to which this activity extends, is lacking. However, this situation has begun to change. Bloch *et al.* (2014) showed that upper crustal seismicity in the forearc region of the Nazca subduction zone defines a deep reverse structure explained by a rheological change from brittle to ductile across a boundary that mechanically separates rigid upper crust from ductile lower crust. This structure has been confirmed by Storch *et al.* (2016) and Schmelzbach *et al.* (2016). These structures define a triangular zone in the forearc-slab system, which could be interpreted as a rigid wedge, and that has resisted the westward movement of crustal material coming from the shortened eastern foreland. This concept is similar to that previously described by Tassara (2005).

A more enigmatic topic is the role that these structures play in the ascent of fluids towards the upper crust and how the migration of these fluids is influenced by the stress state of the crust. The presence of earthquake clusters in different levels of the upper crust, which are spatially related to the structures mentioned above, leads us to think that these clusters may be caused by structural complexities associated with the WFFS and/or fluid migration. This article focuses on upper crustal seismotectonic activity in order to identify the origins of the clusters and their relationship with the state of stress in the upper plate. To characterize the signals caused by the sources, we analyse high-quality seismic data from the WFFS that were recorded between 2005 and 2009. Studying these processes, especially fluid migration and stress transference, gives us a viewpoint on the role that these phenomena have played in triggering seismic activity in the upper crust.

2 SEISMICITY

2.1 Experiment set up and data

To monitor the seismicity, a temporary seismic network covering an area of approximately 50 × 50 km was installed in November 2005 (Fig. 1). This network recorded continuously until 2012. The network was located at approximately 21°S because of a series of existing geophysical observations at this latitude (ANCORP Working Group 1999; Yuan *et al.* 2000; ANCORP Working Group 2003).

The seismic short-period network consisted of twelve 3-component instruments (1 Hz MARK L4-3-D seismometers with EDL PR6-24 data loggers), which recorded continuously at a sample rate of 200 or 100 Hz, respectively, and at high/low gain.

Recording activities were concentrated around the WFFS. To date, observations collected through November 2009 have been processed. Study of these data has yielded detailed information on seismicity, stress distribution, and crustal structures in and near the WFFS. The continuous data streams, recorded in miniseed format, were processed, resulting in the detection of 1427 events within the network and in its immediate vicinity.

The events were determined using an improved technique described by Lomax *et al.* (2000), namely nonlinear localization (NonLinLoc; see Supporting Information Section A1). The crustal model used in the computations is a regional 2-D VP model (Fig. 2) inferred from active seismics (Lüth 2000). The V_S were calculated using a ratio of $V_P/V_S = 1.78$. The combination of these two factors, nonlinear location and a region-specific 2-D velocity model, permitted the reduction of maximum errors in event locations to

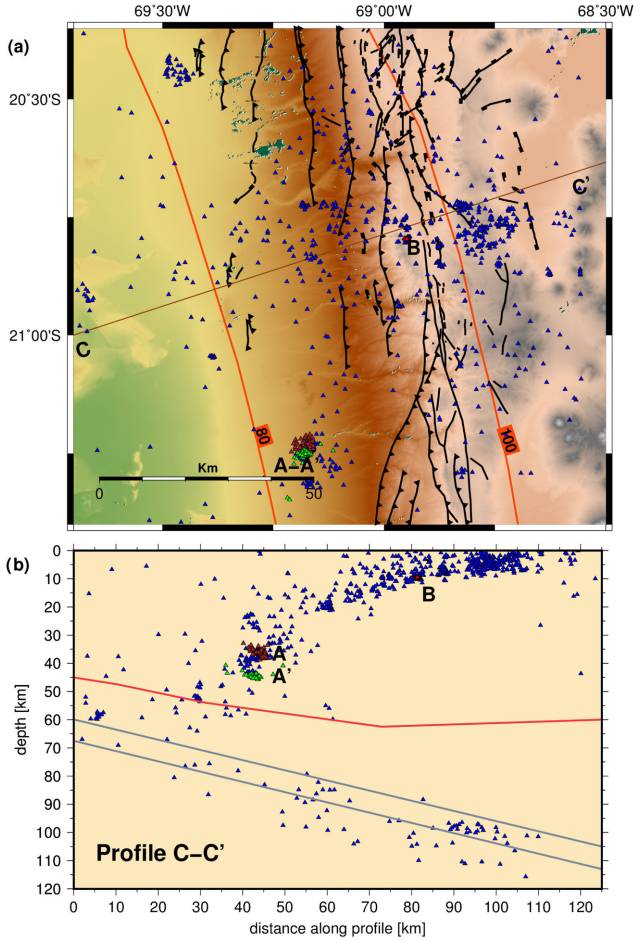

Figure 3. Local seismicity around the West Fissure Fault System (WFFS) detected during 48 months of monitoring (11/2005–11/2009). On the map (a), the WFFS is shown as black lines after Reutter *el al.* (1994), Camus (2003), SERNAGEOMIN (2003) and Victor *et al.* (2004). Earthquake locations are represented by blue triangles; seismicity related to Nazca plate subduction is shown in part. The orange lines indicate the 80- and 100-km isodepth lines of seismicity in the Wadati-Benioff zone after Schurr (2000). The brown line (C–C′) indicates the profile N72E, which is perpendicular to the isodepth lines. The clusters are indicated by A (in brown), A′ (in green) and B (in red). The cross section (b) shows earthquake locations along the C–C′ profile. The red line indicates the continental Moho and the grey lines indicate the top and bottom of the Nazca plate (both after Yuan *et al.* 2000).

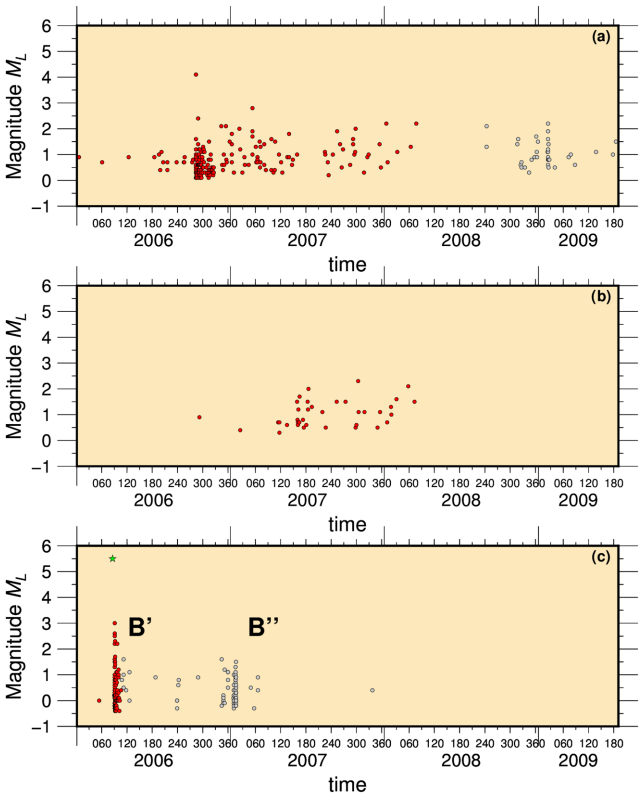

Figure 4. The magnitude of seismicity associated with the clusters, shown as a function of time. Panels (a) and (b) show the distributions in the subclusters A and A′, respectively. Panel (c) shows the distribution in the swarm B; the capital letters B′ and B″ indicate that the swarm can be divided into two phases. The grey dots show the events that are not included in the subsequent cluster analysis. The green star in panel (c) indicates the occurrence of an event with $M_L = 5.5$ near the Nazca plate.

less than 2 km in ∼95 per cent of the data. Location errors were less than 1 km for the analysed clusters (Supporting Information Fig. S6).

2.2 Results

Analysis of continuous waveforms identified 1427 local seismic events. The magnitudes of these events are between $-0.7 \leq M_L \leq 4.1$, and their focal depths range from ∼4 km above sea level to ∼110 km below sea level. Only a few earthquakes from the subduction zone were included in this study because our primary goal was to investigate upper crustal seismicity.

The temporary seismic network increased the number of events detected in the area by ∼53 times, considering that the Global Seismographic Network recorded 147 events in this area between 1960 and January 2015 (Fig. 1). Installation of the local network also improved the possibility of determining the focal mechanisms of earthquakes within the study region, given that previous information on this subject was practically non-existent.

Spatial analysis of the data permits us to infer that the upper crustal microseismicity is partly associated with the surface traces of known branches of the WFFS (Fig. 3a). Projecting the locations of these events onto a W–E section shows that the seismicity has a distinct lower boundary, consistent with that found by Bloch *et al.* (2014). This boundary is clearly dipping to the west (Fig. 3b).

Two clusters were detected in the central and southwestern parts of the study area. These clusters display a complex evolution in space and time, evidencing different phases of activity.

The SW cluster was separated into two subclusters (A and A′) at 35 and 40 km depth, respectively. Subcluster (A) consists of 224 events occurring between 2006 January 6 and 2009 July 4, with a magnitude distribution of $0.1 \leq M_L \leq 4.1$ (Figs 4a and b). Subcluster (A′) consists of 38 events occurring between 2006 October 19 and 2008 March 13; its magnitude distribution is $0.3 \leq M_L \leq 2.3$.

The central cluster (B) is located at ∼9 km depth and includes 185 events occurring between 2006 February 23 and 2007 December 4; its magnitude distribution is $-0.4 \leq M_L \leq 3.0$ (Fig. 4c). It can be separated into two phases (B′ and B″). This cluster exhibits characteristics of an earthquake swarm (Wigger *et al.* 2007); most of the events associated with it have very high cross-correlation coefficients (greater than 0.8), but there is no large event associated with the sequence. As the waveform similarity is quite high, these events must be located within a small volume. The maximum interevent distance is on the order of 1 km. It may also be

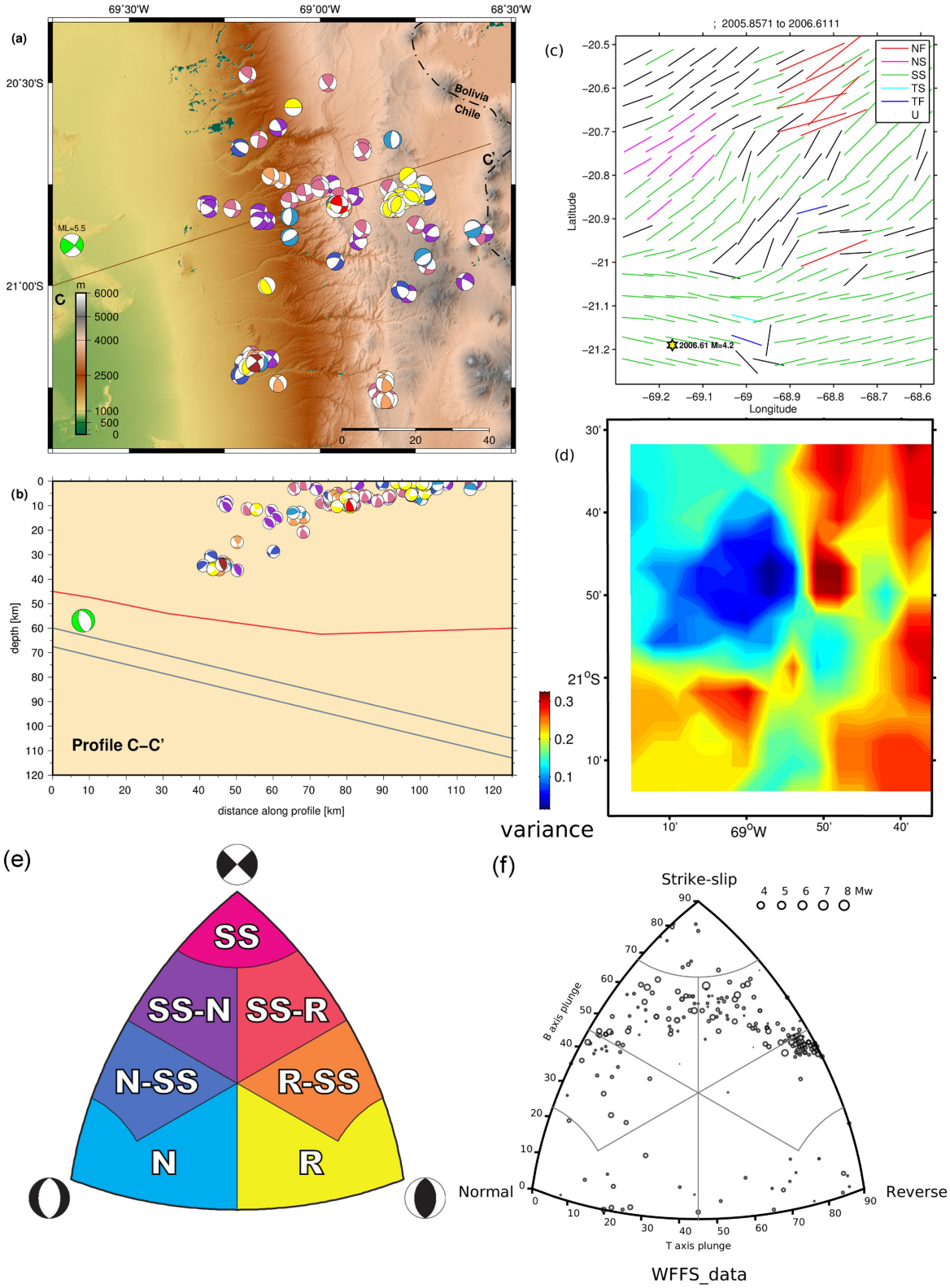

Figure 5. (a) Map that shows focal mechanisms (FMs) in the study region [see (e) for colour code]. The map view also shows in green an $M_L = 5.5$ event near the Nazca plate that occurred 72 hr before swarm activity began. The brown line (C–C′) indicates the N72E profile. (b) Cross-section that shows FMs projected on the C–C′ profile. The red and grey lines indicate the continental Moho and the top and bottom of the Nazca plate, respectively (both after Yuan *et al.* 2000). (c) Stress map that shows the orientation of the maximum horizontal stress σ_{Hmax} for the zone, using colours to indicate the type of faulting regime according to Zoback (1992) (NF: normal fault, NS: normal-strike, SS: strike-slip, TS: thrust-strike, TF: thrust fault, U: unknown). (d) Plot showing the variance of the stress map at each node. (e) Focal mechanism classification diagram, according to Álvarez-Gómez (2009)—SS, strike-slip; SS-N, strike-slip with normal component; SS-R, strike-slip with reverse component; N-SS, normal with strike-slip component; R-SS, reverse with strike-slip component; N, normal; R, reverse. (f) Classification of FMs for seismic events occurring within the WFFS.

Table 1. Stress tensor parameters.

Zone	Nev[a]	σ_1^*	σ_2^*	σ_3^*	φ^b	*Var*[c]	β^d	Type[e]
West Fissure	214	235.5/12.2	122.7/60.6	331.5/26.2	0.43 ± 0.06954	0.18	39.55	SS

[a]Number of events in inversion.
*Stress components (Azimut/plunge).
[b]Stress ratio $\varphi = (\sigma_2 - \sigma_3)/(\sigma_1 - \sigma_3)$.
[c]Variance or measure of stress homogeneity.
[d]Average misfit angle between the predicted and observed slip directions.
[e]Faulting type classification according to Zoback (1992): SS, strike-slip.

speculated that this swarm was triggered by a magnitude $M_L = 5.5$ event occurring nearby on the Nazca plate; both events are very close in time.

The temporal continuity of these different clusters could be related to the migration of fluids through the crust. A detailed study of these clusters and their relation to fluid flow from the lower to the upper crust will be the subject of the following sections.

3 CHARACTERIZATION OF THE WFFS

3.1 Focal mechanisms

A total of 214 focal mechanisms and a posterior stress tensor analysis were used to characterize the WFFS in terms of its kinematic behaviour. Cursory examination of Figs 5(a) and (b) show considerable variation among the calculated focal mechanisms and suggests that these events lack any well-defined trend. However, a detailed analysis shows that a majority of the events have oblique focal mechanisms with many of them showing substantial components of strike-slip movement, particularly at shallow depths (Figs 5c–f). Additionally, study of the hypocentres and nodal planes permits spatial correlation of some of the shallower focal mechanisms to faults with surface expressions in the Precordillera (Reutter *et al.* 1994; Victor *et al.* 2004; Farías *et al.* 2005).

Another important point is that the seismic activity is more or less continuous from the Nazca contact to the upper crust. However, no reliable evidence permits association of this seismicity with a reverse fault, as might be inferred from the presence of the Altiplano uplift. These events likely indicate an important zone of weakness in the intermediate and deeper parts of the continental crust, probably associated with the brittle-ductile transition (Figs 2b and 4b).

3.2 Stress tensor analysis

The focal mechanisms were also used as a tool to determine the direction and shape of the stress tensor according to the algorithm of Michael (1987) implemented through the MATLAB-based ZMAP software package (Wiemer 2001).

Geological studies in the area show that N–S trending thrust faults and monoclinal flexures dominate at the base and the western flank of the Precordillera, indicating W–E directed shortening, whereas the eastern flank of the Precordillera is dominated by normal and strike-slip faults indicating NW–SE directed extension with dextral strike-slip motion along N–S trending faults (Janssen *et al.* 2002; Victor *et al.* 2004).

Owing to the complex tectonic frame and the considerable variation in focal mechanisms, the procedure for calculating stress tensors included the complete catalogue of focal mechanisms for the study area. Although division of the study area into zones using tectonic context and depth as criteria was initially considered, the results do not change greatly if we consider a single zone. Another important reason to use a single solution for the zone is that the misfit angle β, which reflects the degree of homogeneity of the stress field within a given volume, is ∼40° (Table 1), which provides a valid fit to a single deviatoric stress tensor (Michael *et al.* 1990; Michael 1991).

The resulting stress tensor has a horizontal σ_1 (Fig. 6; Table 1), compatible with the regional plate motion direction (Somoza 1998). The σ_2 is practically in the vertical direction and has a stress ratio $\varphi \sim 0.43$, indicating a strike-slip regime in this zone. The σ_3 has an NNW–SSE direction, which matches the strike of different tectonic signatures that are present on both sides of the mean trace of the WFFS (David *et al.* 2002; Janssen *et al.* 2002; Victor *et al.* 2004).

Conversely, the stress map was calculated by ZMAP (Wiemer 2001) on a ∼5 × 5 km horizontal grid with the 15 nearest mechanisms in plane view inverted at each grid node. The resulting map of the maximum horizontal stress σ_{Hmax} is shown in Fig. 5(c), and the variance associated with this inversion is shown in Fig. 5(d).

The results show no further changes in the stress directions and faulting types. Thus, the stress directions show a high coherence with the regional plate motion (∼WSW–ENE), consistent with Somoza (1998). Some rotation to the north (that is, parallel to the trench) indicates slip partitioning. Strike slip is the dominant faulting regime in this zone, which is in agreement with the result of our stress tensor analysis.

These observations indicate that transference of stress from the coupled zone to the upper crust in the interseismic cycle is manifested as seismic activity. Therefore stress release presently occurs as inelastic deformation clearly located in deep zones of weakness, particularly reactivated ancient structures in the Precordillera.

4 ANALYSIS OF SEISMIC CLUSTERS ASSOCIATED TO WFFS

In addition to structural and tectonic features, we observe that the locations associated with seismic clusters have important differences, as well as similarities (for further information, see the supplementary material). Thus, the central cluster B has the characteristics of an earthquake swarm; it lacks any large event and has a closed distribution in space and time (Fig. 4c and Supporting Information Fig. S7a; Supporting Information Section A7). Conversely, the SW cluster has characteristics that are typical of earthquake clusters at tectonic plate boundaries; it contains large events, has *b*-values consistent with a tectonic origin and persists over an extended period (Fig. 4a and Supporting Information Fig. S4b; Supporting Information Section A6.1).

The similarities among these clusters permit us to infer that they may have a common origin. The different analyses we performed indicate that background activity is very low, meaning that the activity we observed is likely not simply due to aftershock sequences (Supporting Information Figs S5a and b; Supporting Information

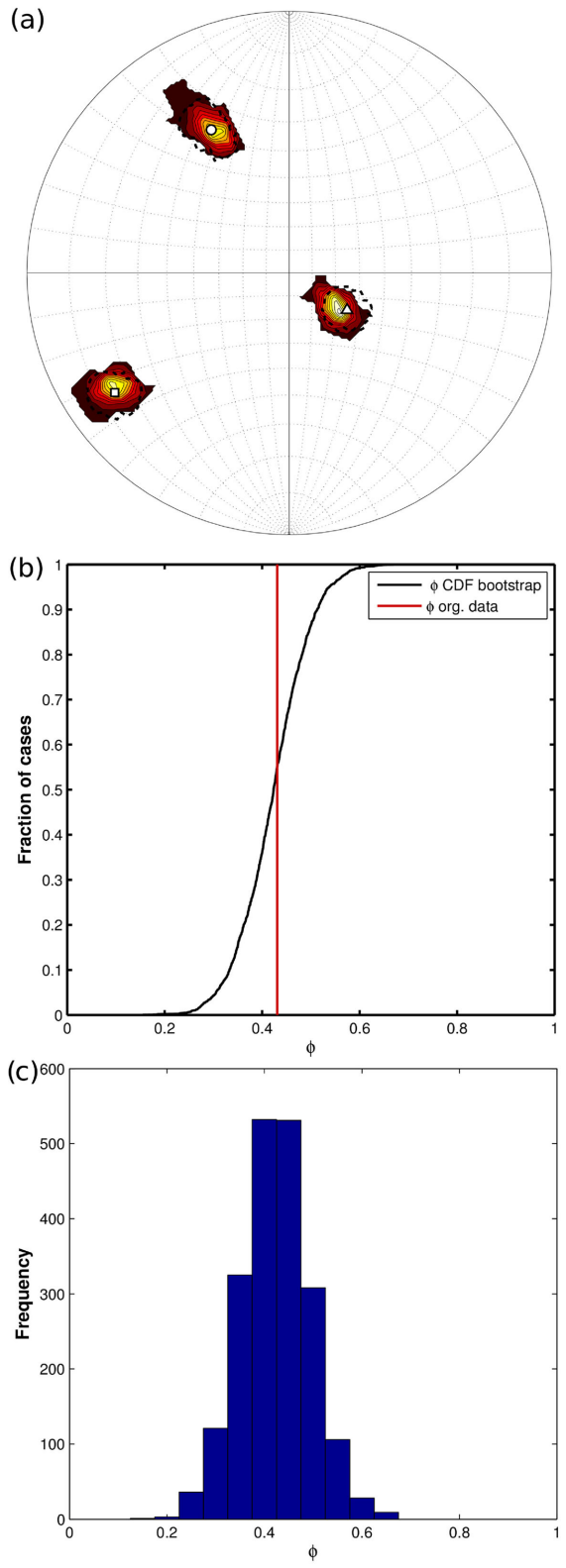

Figure 6. Stress tensor parameter according to Michael (1987). Panel (a) shows the results of stress tensor inversion (square: σ_1, triangle: σ_2 and circle: σ_3). The confidence area, resulted from the stress tensor inversion, are indicated by the isolines of colours surrounding each symbol (brown and white indicate lowest and best confidence, respectively); panel (b) shows the φ-ratio of relative stress magnitudes as a cumulative density function; panel (c) shows the φ-ratio of relative stress magnitudes as a histogram.

Section A6.2). We note that the magnitudes of the main shocks are not large enough to maintain long-term seismic activity (Fig. 4). Thus, a non-stationary external forcing (e.g. fluids) may explain the patterns in the observed seismicity. This hypothesis can be investigated by analysing the non-DC component of the moment tensor (Supporting Information Fig. S1). This tensor shows values ∼8 per cent. Although this value is not very high, it does not rule out the possibility that fluids play a role in generating the seismicity associated with this cluster (see Supporting Information Section A4 for further information).

Conversely, the spatial and moment tensor analyses confirm that the earthquakes are nearly all coplanar, and define clear rupture planes (Supporting Information Figs S1–S8; Supporting Information Sections A4 and A7). Additionally, the active areas show phases with an almost constant rate of growth separated by phases with rapid increase in this growth rate (Supporting Information Figs S9–S11; Supporting Information Section A8). We also find that the main shocks triggered aftershocks, which preferentially occur at the edge of the rupture zones of the preceding event (Supporting Information Figs S12 and S13; Supporting Information Section A8). Analysis of the spreading of the active area also show that this behaviour, in which earthquakes preferentially occur at the edges of preceding ruptures, are not exclusive to the aftershocks. Instead, this behaviour appears throughout the seismic activity of the swarm and subcluster A.

The spatial and spatio-temporal analyses reveal that this behaviour results from stick-slip fracture propagation (Supporting Information Sections A7 and A8). Stick-slip rupture growths can have dynamic as well as structural causes. One possible mechanism is dynamic pore generation in a fluid-permeated fault, where the fluid is assumed to flow out of a localized high-pressure fluid compartment with the onset of earthquake rupture (Yamashita 1999). Another mechanism might be structural inhomogeneities combined with viscoelastic coupling due to magma-filled dikes (Hill 1977). The spatio-temporal migration reveals that fluid movement is a possible mechanism for triggering the seismic activity, as shown by the temporal migration of hypocentres, which coincide with curves that describe the hypothetical migration of the pressure front from the fluid sources (Fig. 7).

The key to understanding these processes can be obtained from comparison with results from other geophysical methods. We found that the swarm and subcluster A are spatially correlated with geophysical anomalies found by previous studies. The swarm is located directly above a singular high conductivity anomaly (Fig. 8), which was interpreted as a fluid migration zone by Brasse *et al.* (2002). Subclusters A and A′ are associated with a high reflectivity zone seen in seismic images (Fig. 9), which was also interpreted as a fluid migration zone by Yoon *et al.* (2009).

5 DISCUSSION

At the latitude of our study (21°S), seismic reflection studies and geophysical experiments show the presence of a <30 km deep, west-dipping reflector below the Precordillera (Bloch *et al.* 2014; Schmelzbach *et al.* 2016; Storch *et al.* 2016). Additionally, there is a major reflector—the Quebrada Blanca Bright Spot (QBBS)—that is associated with a low-velocity zone and *P*- to *S*-wave conversions and corresponds to the upper boundary of a domain with high conductivity values and high Poisson's ratios (ANCORP Working Group 2003). ANCORP Working Group (2003) favoured the idea that the QBBS is a petrophysical feature related to the presence of

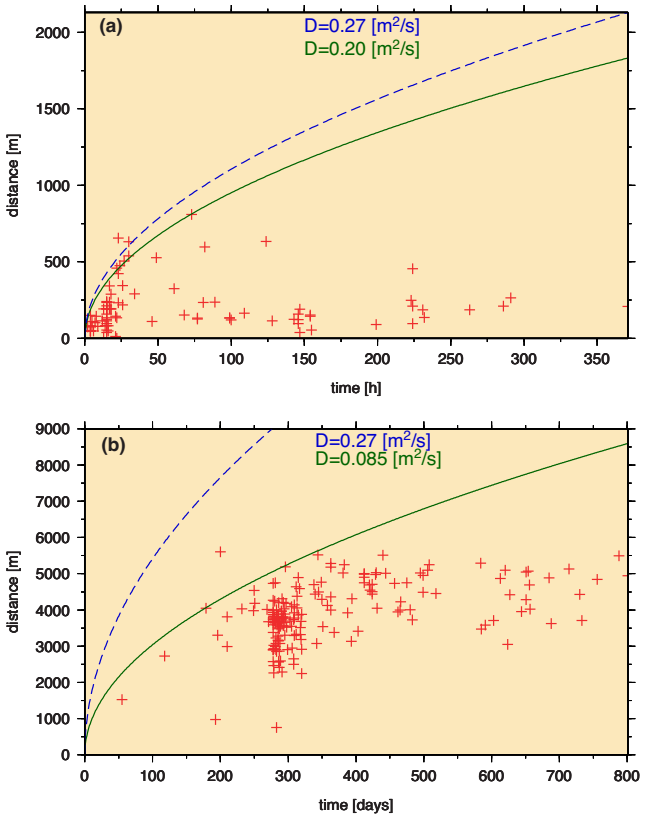

Figure 7. Hypocentre distances measured from the first event as a function of the earthquake occurrence times for (a) the swarm and (b) subcluster A. The green line refers to the theoretical position of the propagating pore pressure front, assuming hydraulic diffusivities $D = 0.20$ m^2 s^{-1} and $D = 0.085$ m^2 s^{-1} for the swarm and subcluster A, respectively. The blue line represents the pore pressure front for the Vogtland swarm (Hainzl & Ogata 2005).

fluids, melts, or mafic intrusions in a felsic country rock. Victor *et al.* (2004) suggest that the western termination of this reflector corresponds to the downdipping end of the west-vergent thrust that crops out in Altos de Pica area.

This discontinuity can be traced farther east, beneath the Altiplano and Eastern Cordillera at depths between 15 and 30 km, where it is called the Altiplano low-velocity zone (here, LVZ; Wigger *et al.* 1994; Yuan *et al.* 2000). The LVZ is likely related to the mid-crustal brittle-ductile transition, where the rigid upper

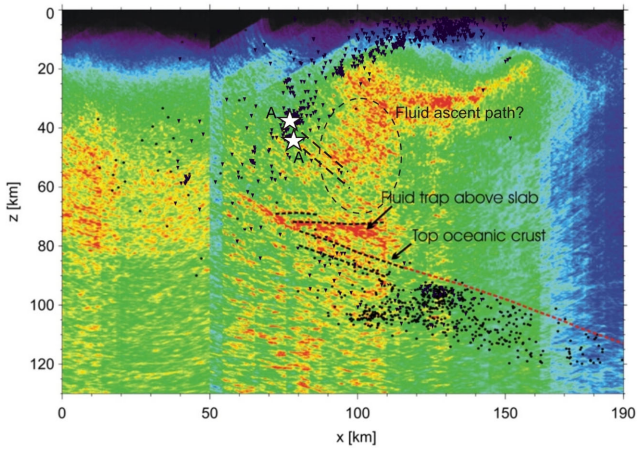

Figure 9. The seismicity (black dots) is overimposed to the Yoon's model (Yoon *et al.* 2009). It is clear to see that the seismicity is a boundary for the high reflectivity zones (red colours). The location of the subclusters A and A′ (white stars) are also overimposed.

crust decouples mechanically from the ductile lower crust (Yuan *et al.* 2000; ANCORP Working Group 2003).

The distribution of crustal microseismicity in the study area confirms the existence of the west-dipping boundary proposed by Bloch *et al.* (2014). This boundary may be related to changes in the crustal rheology; that is, this plane may represent the brittle-ductile boundary in the crust mentioned above. The good correlation between the boundary defined by this seismicity and the 350 °C (Springer 1999) supports the idea that this boundary represents a rheological feature of the crust (Fig. 10). The good agreement between the LVZ and the eastward prolongation of this west-dipping structure also confirms this idea. The west-dipping boundary in seismicity also represents a boundary for high-reflectivity zones identified in the model proposed by Yoon *et al.* (2009, their fig. 9).

In terms of the kinematic characterization of the WFFS from the Pliocene to the present, Victor *et al.* (2004) found evidence of N–S strike-slip motion and pull-apart basin formation with NW–SE extension bordering the Salar de Huasco, in the Altos de Pica region, which began in the late Pliocene. The focal mechanisms of the Aroma and Chusmiza earthquakes and the swarm event identified in this study agree well with the strike-slip deformation observed in geological studies in the Altos de Pica region (Victor *et al.* 2004; Farías *et al.* 2005). Therefore, geological and seismological evidence are in agreement with the results obtained from

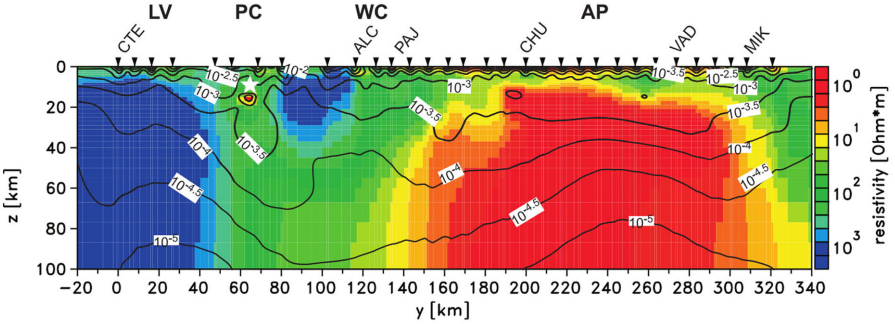

Figure 8. Result of the 2-D MT resistivity inversion model. Superimposed are isolines of sensitivities for this model. The sensitivities shown here were calculated by summing up columnwise the error-weighted absolute values of the sensitivity matrix (Brasse *et al.* 2002). The white star indicates the location of the swarm, which is found directly above the high conductivity zone related to the West Fissure Fault System. LV, Longitudinal Valley; PC, Precordillera; WC, Western Cordillera; AP, Altiplano. Magnetotelluric stations: CTE, ALC, PAJ, CHU, VAD and MIK.

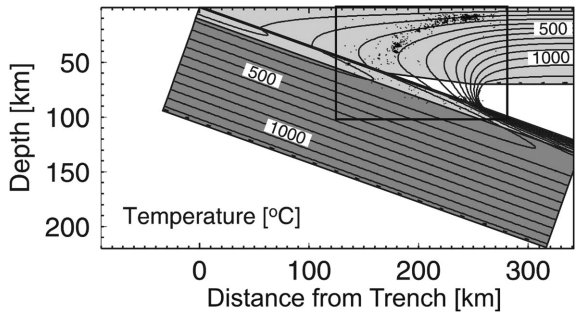

Figure 10. The seismicity is overimposed to the Springer's model (Springer 1999). The seismicity is clearly related to the isotherm of 350 °C, which support the hyphotesis that the seismicity represent a rheological transition (brittle-ductile) in the crust.

inversion of the stress tensor over our study area, which shows strike-slip motion with NW–SE extension (Fig. 6). Thus, multiple lines of evidence indicate that the strike-slip stress regime has been active over several million years, favouring the creation and activation of the transcurrent structures of the Precordillera.

In contrast, north of Aroma, David *et al.* (2002) showed that the deep forearc of the Arica region (18°–19°S) is undergoing ENE–WSW shortening associated with the activity of east-vergent thrusting. The results from this earlier study coincide with the direction of σ_1 in the inversion of the stress tensor for our study area. Thus, the maximum stress axis calculated for our study area is almost parallel to the present-day plate convergence direction. A similar pattern is found in the P-axis mechanism of the Aroma earthquake (Legrand *et al.* 2007), the Pliocene-Recent σ_1 direction estimated in Altos de Pica (Victor *et al.* 2004), and the maximum stress axis calculated by David *et al.* (2002) in the Arica region.

The kinematic behaviour of the WFFS may be the result of the following possible causes. (a) Oblique eastward movement of the rigid forearc (compared with the perpendicular trench direction) could account for the observed partitioning of deformation phenomena within the study area. (b) Perturbation of the vertical lithospheric stress σ_V due to the weight of the topography (Tibaldi *et al.* 2009). Under this hypothesis, the σ_V value would be higher than the minimum horizontal stress σ_{Hmin} assuming the value of σ_2. This change in the horizontal stress would permit the partitioning deformation phenomenon in the shallow zone. Previous studies (e.g. Meijer *et al.* 1997; Tibaldi *et al.* 2009) have shown that relatively slight increases of average altitude in mountain belts are sufficient to produce changes in dominant faulting style.

Therefore, the state of stress of the convergence margin of northern Chile has always been related to compression, and according to the explanation above, the strike-slip regime is restricted to the highest areas as a result of local stresses imposed by the thickened crust. Similar results were reported by Yoshida *et al.* (2015), who found that strike-slip faulting stress regimes are dominant beneath high-altitude regions. They also described the correlation between the stress regime and the surface topography as resulting from gravitational forces caused by topography.

Analysis of the clustered seismic events revealed that the swarm and clusters are coplanar (Supporting Information Figs S7 and S8; Supporting Information Section A6). The *b*-values associated with subclusters A and A′ are typical for tectonic plate boundaries (Supporting Information Fig. S4b; Supporting Information Section A6.1), where $0.7 \leq b \leq 1.1$ (Karnik *et al.* 1986; Mittag 2000). However, in the case of the swarm, the *b*-value is slightly low, which can be explained by seismic moment accumulation (Supporting Information Fig. S4a; Supporting Information Section A6.1).

The low values for the background seismicity indicate that only part of the events can be related to aftershock sequences (Supporting Information Fig. S5; Supporting Information Section A6.2). An important amount of the observed seismicity cannot be directly related to aftershocks, because the seismic activity in the swarm and subcluster A occur over a long time period and the magnitudes for the largest events are very low to maintain this behaviour over time (Fig. 4).

Therefore, the main part of the swarm and subcluster A seismic activity results from stick-slip fracture propagation, which may be caused by dynamic pore creation along a fluid-permeated fault. This hypothesis is supported by the observed spatio-temporal migration of seismic event hypocentres, which are in agreement with those expected from propagation of the pressure front of a fluid source. The good spatial correlation that the swarm and subcluster A have with areas that were interpreted as fluid migration zones by previous research also tend to confirm our hypothesis.

6 CONCLUSIONS

Important clusters of earthquakes were found in different levels of the upper crust, spatially related to the reverse structure previously described by Bloch *et al.* (2014), Schmelzbach *et al.* (2016) and Storch *et al.* (2016). This structure may be related to changes in the rheological behaviour of the crust with depth (specifically the brittle-ductile boundary, which mechanically separates the rigid upper crust from the ductile lower crust).

Solving for the regional stress field shows that the zone is in a strike-slip regime. Therefore, the state of stress in the convergent margin is related to compression, supporting the idea of a rigid wedge moving eastward, obliquely to the overall convergence direction, along the decoupled surface associated with the structure described above. The strike-slip regime would then be a manifestation of local forces associated with the highest areas in the Andes that would rotate the intermediate stress axis to a vertical position. Thus, the deviatoric stress magnitudes caused by the topography play an important role in this area. The role of topography is not only seen in this study but was also previously identified by Yoshida *et al.* (2015).

Moreover, the presence of this west-dipping boundary may favour the migration of the fluids to shallower levels in the upper crust. In this hypothesis, this structure acts like a highway along which the fluids can ascend. Thus, it is possible to see that the clustered seismicity is closely related to the deeper limit of the seismicity, which define this lower boundary.

Finally, this hypothesis is also supported by the close relationship between the WFFS and the porphyry-copper system, where mineralization and alteration have progressed for millions of years and are undoubtedly related to the presence of fluids.

ACKNOWLEDGEMENTS

We thank the Deutsche Forschungsgemeinschaft (PAK 262, Sh55/10-1.1) for funding. PS has been also supported by the FONDAP (CIGIDEN) 15110017 grant. Part of the instruments were provided by the GIPP of the GeoForschungszentrum Potsdam. We also want to thank to Dr Guillermo Chong (Universidad Católica del Norte, Chile) and Juan Thomas (Universidad de Chile) for broad

support in Chile. The authors also thank to Eiichi Fukuyama and the anonymous reviewers for careful revision of the manuscript.

REFERENCES

Álvarez-Gómez, J.A., 2009. Tectónica Activa y Geodinámica en el Norte de Centroamérica, *PhD thesis,* Universidad Complutense de Madrid, Madrid.

ANCORP Working Group, 1999. Seismic reflection image revealing offset of Andean subduction-zone earthquake locations into oceanic mantle, *Nature,* **397,** 341–344.

ANCORP Working Group, 2003. Seismic imaging of an active continental margin and plateau in the central Andes (Andean Continental Research Project 1996 (ANCORP'96)), *J. geophys. Res.,* **108**(B7), 2328, doi:10.1029/2002JB001771.

Bloch, W., Kummerow, J., Salazar, P., Wigger, P. & Shapiro, S., 2014. High-resolution image of the North Chilean subduction zone: seismicity, reflectivity and fluids, *Geophys. J. Int.,* **197,** 1744–1749.

Brasse, H., Lezaeta, P., Rath, V., Schwalenberg, K., Soyer, W. & Haak, V., 2002. The Bolivian Altiplano conductivity anomaly, *J. geophys. Res.,* **107**(B5), doi:10.1029/2001JB000391.

Camus, F., 2003. *Geología de los sistemas porfídicos de los Andes de Chile,* Servicio Nacional de Geología y Minería.

David, C., 2007. Comportamiento actual del ante-arco y del arco del codo de Arica en la orogénesis de los Andes centrales, *PhD thesis,* Universidad de Chile.

David, C., Martinod, J., Comte, D., Hérail, G. & Haessler, H., 2002. Intracontinental seismicity and Neogene deformation of the Andean forearc in the region of Pica (18.5°–19.5°S), in *5th International Sysposium on Andean Geodynamics,* Ins. de Rech. pour le Dév. (IRD), Tolouse, France.

Delouis, B. & Legrand, D., 2007. Mw 7.8 Tarapaca intermediate depth earthquake of 13 June 2005 (northern Chile): fault plane identification and slip distribution by waveform inversion, *Geophys. Res. Lett.,* **34,** L01304, doi:10.1029/2006GL028193.

Farías, M., Charrier, R., Comte, D., Martinod, J. & Hérail, G., 2005. Late Cenozoic deformation and uplift of the western flank of the Altiplano: evidence from the depositional, tectonic, and geomorphologic evolution and shallow seismic activity (northern Chile at 19°30′S), *Tectonics,* **24,** TC4001, doi:10.1029/2004TC001667.

Haberland, C. & Rietbrock, A., 2001. Attenuation Tomography in the Western Central Andes: a detailed insight into the structure of a magmatic arc, *J. geophys. Res.,* **106**(B6), 11 151–11 167.

Hainzl, S. & Ogata, Y., 2005. Detecting fluids signals in seismicity data through statistical earthquake modelling, *J. geophys. Res.,* **110,** B05S07, doi:10.1029/2004JB003247.

Heit, B., 2005. *Teleseismic Tomographic Images of the Central Andes at 21°S and 25.5°S: An inside look at the Altiplano and Puna plateaus, Scientific Technical Report STR06/05*, 139 pp. GeoForschungsZentrum Potsdam, Germany.

Hill, D.P., 1977. A model for earthquake swarms, *J. geophys. Res.,* **82,** 1347–1352.

Hoffmann-Rothe, A., Kukowski, N., Dresen, G., Echtler, H., Oncken, O. & Klotz, J., 2006. Oblique convergence along the Chilean margin: partitioning, margin-parallel faulting and force interaction at the plate interface, in *The Andes,* pp. 125–146, eds Oncken, O., Chong, G., Franz, G., Giese, P., Götze, H.-J., Ramos, V.A., Strecker, M. & Wigger, P., Springer-Verlag.

Janssen, C., Hoffmann-Rothe, A., Tauber, S. & Wilke, H., 2002. Internal structure of the Precordillera fault system (Chile) - insights from structural and geophysical observations, *J. Struct. Geol.,* **24,** 123–143.

Jarrard, R.D., 1986a. Relations among subduction parameters, *Rev. Geophys.,* **24**(2), 217–284.

Jarrard, R.D., 1986b, Terrane motion by strike-slip faulting of forearc slivers, Geology, **14,** 780–783.

Karnik, V., Schenkova, Z. & Schenk, V., 1986. Time pattern of the swarm of December 1985-March 1986 in West Bohemia, in *Proceedings of the Workshop in Lazne: Earthquake Swarm 1985/86 in Western Bohemia,* pp. 328–342.

Legrand, D., Delouis, B., Dorbath, L., David, C., Campos, J., Marquéz, L., Thompson, J. & Comte, D., 2007. Source parameters of the Mw = 6.3 Aroma Crustal earthquake of July 24, 2001 (northern Chile), and its aftershock sequence, *J. S. Am. Earth Sci.,* **24,** 58–68.

Lindsay, D.D., Zentilli, M. & Rivera, A.J., 1995. Evolution of an active ductile to brittle shear system controlling mineralization at Chuquicamata porphyry copper deposit, Northern Chile, *Int. Geol. Rev.,* **37,** 945–958.

Lomax, A., Virieux, J., Volant, P. & Berge, C., 2000. Probabilistic earthquake location in 3D and layered models: introduction of a Metropolis-Gibbs method and comparison with linear locations, in *Advances in Seismic Event Location,* pp. 101–134, eds Thurber, C.H. & Rabinowitz, N., Kluwer.

Lüth, S., 2000. Results of wide-angle investigations and crustal structure along a traverse across the central Andes at 21 degrees south. *PhD thesis,* Institute of Geology, Geophysics and Geoinformatics, Free University of Berlin, Berliner Geowissenschaftliche Abhandlungen, Band 37, Reihe B, Berlin, Germany.

Meijer, P.Th., Govers, R. & Wortel, M.J.R., 1997. Forces controlling the present-day state of stress in the Andes, *Earth planet. Sci. Lett.,* **148,** 157–170.

Michael, A.J., 1987. Use of focal mechanisms to determine stress: a control study, *J. geophys. Res.,* **92,** 357–368.

Michael, A., 1991. Spatial variations in stress within the 1987 Whittier Narrows, California, aftershock sequence: new techniques and results, *J. geophys. Res.,* **96**(B4), 6303–6319.

Michael, A., Ellsworth, W. & Oppenheimer, D., 1990. Coseismic stress change induced by the 1989 Loma Prieta, California earthquake, *Geophys. Res. Lett.,* **17**(9), 1441–1444.

Mittag, R., 2000. Statistical investigations of earthquake swarms within the Vogtland/NW-Bohemia area, *Studia Geophys. Geod.,* **44,** 465–474.

Ossandón, G., Fréraud, R., Gustafson, L., Lindsay, D. & Zentilli, M., 2001. Geology of the Chuquicamata mine: a progress report, *Econ. Geol.,* **96,** 249–270.

Peyrat, S. *et al.*, 2006. Tarapacá intermediate-depth earthquake (Mw 7.7, 2005, northern Chile): a slab-pull event with horizontal fault plane constrained from seismologic and geodetic observations, *Geophys. Res. Lett.,* **33,** L22308, doi:10.1029/2006GL027710.

Reutter, K.-J., Scheuber, E. & Helmcke, D., 1991. Structural evidence of orogen-parallel strike slip displacements in the Precordillera of northern Chile, *Geologische Rundsch.,* **80,** 135–153.

Reutter, K.-J., Döbel, R., Bogdanic, T. & Kley, J., 1994. Geological map of the central Andes between 20°S and 26°S, in *Tectonics of the Sourthern Central Andes,* eds Reutter, K.-J., Scheuber, E. & Wigger, P., Springer Verlag.

Reutter, K.-J., Scheuber, E. & Chong, G., 1996. The Precordilleran fault system of Chuquicamata, Northern Chile: evidence for reversals along arc-parallel strike-slip faults, *Tectonophysics,* **259,** 213–228.

Schmelzbach, C., Kummerow, J., Wigger, P., Reshetnikov, A., Salazar, P. & Shapiro, S.A., 2016. Microseismic reflection imaging of the Central Andean crust, *Geophys. J. Int.,* **204**(2), 1396–1404.

Schurr, B., 2000. *Seismic Structure of the Central Andean Subduction Zone from Local Earthquake Data, Scientific Tecnical Report STR01/01*, 125 pp. GeoForschungsZentrum Potsdam, Germany.

SERNAGEOMIN, 2003. *Mapa Geológico de Chile: versión digital, Publicación Geológica Digital No. 4 (CD-ROM versión 1.0, 2003),* Servicio Nacional de Geología y Minería.

Somoza, R., 1998. Updated Nazca (Farallon) – South America relative motions during the last 40 My: implications for mountain building in the central Andean region, *J. S. Am. Earth Sci.,* **11**(3), 211–215.

Springer, M., 1999. Interpretation of heat-flow density in the Central Andes, *Tectonophysics,* **306,** 377–395.

Storch, I., Buske, S., Schmelzbach, C. & Wigger, P., 2016. Seismic imaging of a megathrust splay fault in the North-Chilean subduction zone (Central Andes), *Tectonophysics,* **689,** 157–166.

Sylvester, A., 1988. Strike-slip faults, *Bull. geol. Soc. Am.,* **100,** 1666–1703.

Tassara, A., 2005. Interaction between the Nazca and South American plates and formation of the Altiplano-Puna plateau: review of a flexural analysis along the Andean margin (15°–34°S), *Tectonophysics,* **399,** 39–57.

Tibaldi, A., Corazzato, C. & Rovida, A., 2009. Miocene-Quaternary structural evolution of the Uyuni-Atacama region, Andes of Chile and Bolivia, *Tectonophysics,* **471**(1–2), 114–135.

Tomlinson, A. & Blanco, N., 1997a. Structural evolution and displacement history of the west fault system, Precordillera, Chile: Part 1, Synmineral history, in *Actas 8th Congreso Geológico Chileno,* Vol. 3, Antofagasta, 1873–1877.

Tomlinson, A. & Blanco, N., 1997b. Structural evolution and displacement history of the west fault system, Precordillera, Chile: Part 2, Postmineral history, in *Actas 8th Congreso Geológico Chileno,* Vol. 3, Antofagasta, 1878–1882.

Victor, P., Oncken, O. & Glodny, J., 2004. Uplift of the western Altiplano plateau: evidence from the Precordillera between 20° and 21°S (northern Chile), *Tectonics,* **23,** TC4004, doi:10.1029/2003TC001519.

Wiemer, S., 2001. A software package to analyze seismicity: ZMAP, *Seismol. Res. Lett.,* **72,** 373–382.

Wigger, P. *et al.*, 1994. Variation of the crustal structure of the Sourthern Central Andes deduced from seismic refraction investigations, in *Tectonics of the Sourthern Central Andes,* pp. 23–48, ed. Reutter, K.-J., Scheuber, E. & Wigger, P., Springer Verlag.

Wigger, P., Kummerow, J., Salazar, P., Asch, G. & Moser, D., 2007. Microseismicity in the West Fissure fault system, Northern Chile, *Geophys. Res. Abstr.,* **9,** 07136.

Woodcock, N., 1986. The role of strike-slip fault systems at plate boundaries, *Phil. Trans. R. Soc.* A, **317,** 13–29.

Yamashita, T., 1999. Pore creation due to fault slip in a fluid-permeated fault zone and its effect on seismicity: generation mechanism of earthquake swarm, *Pure appl. Geophys.,* **155,** 625–647.

Yoon, M., Buske, S., Shapiro, S.A. & Wigger, P., 2009. Reflection Image Spectroscopy across the Andean subduction zone, *Tectonophysics,* **472,** 51–61.

Yoshida, K., Hasegawa, A. & Okada, T., 2015. Spatial variation of stress orientations in NE Japan revealed by dense seismic observations, *Tectonophysics,* **647–648,** 63–72.

Yuan, X., Sobolev, S.V., Kind, R., Oncken, O. & Andes Seismology Group, 2000. New constraints on subduction and collision processes in the central Andes from P-to-S converted seismic phases, *Nature,* **408,** 958–961.

Zoback, M.L., 1992. First- and second-order patterns of stress in the lithosphere: the World Stress Map project, *J. geophys. Res.,* **97,** 11 703–11 728.

SUPPORTING INFORMATION

Supplementary data are available at *GJIRAS* online.

supplementary-material-clean-rev-nov.pdf

Please note: Oxford University Press is not responsible for the content or functionality of any supporting materials supplied by the authors. Any queries (other than missing material) should be directed to the corresponding author for the paper.